Editors' Suggestion Featured in Physics

# Fluctuation-Induced Torque on a Topological Insulator out of Thermal Equilibrium

M. F. Maghrebi,[1,*] A. V. Gorshkov,[2,3] and J. D. Sau[2,4]
[1]Department of Physics and Astronomy, Michigan State University, East Lansing, Michigan 48824, USA
[2]Joint Quantum Institute, NIST/University of Maryland, College Park, Maryland 20742, USA
[3]Joint Center for Quantum Information and Computer Science, NIST/University of Maryland, College Park, Maryland 20742, USA
[4]Condensed Matter Theory Center and Physics Department, University of Maryland, College Park, Maryland 20742, USA

(Received 8 January 2019; revised manuscript received 9 May 2019; published 1 August 2019)

Topological insulators with the time reversal symmetry broken exhibit strong magnetoelectric and magneto-optic effects. While these effects are well understood in or near equilibrium, nonequilibrium physics is richer yet less explored. We consider a topological insulator thin film, weakly coupled to a ferromagnet, out of thermal equilibrium with a cold environment (quantum electrodynamics vacuum). We show that the heat flow to the environment is strongly circularly polarized, thus carrying away angular momentum and exerting a purely fluctuation-driven torque on the topological insulator film. Utilizing the Keldysh framework, we investigate the universal nonequilibrium response of the TI to the temperature difference with the environment. Finally, we argue that experimental observation of this effect is within reach.

DOI: 10.1103/PhysRevLett.123.055901

Three-dimensional topological insulators (TIs) are a new class of matter whose electronic wave functions possess a nontrivial topology [1–6]. While TIs are insulating in the bulk similar to trivial insulators, their surfaces have unconventional properties since they harbor Dirac-like gapless states protected by time-reversal symmetry—the latter is dictated by the bulk state, an example of the correspondence between the bulk and the edge. This new paradigm and its various applications have attracted tremendous interest in recent years. If the time reversal symmetry is weakly broken, for example, by proximity to a ferromagnet or by applying a magnetic field, the topological insulator exhibits a topological magnetoelectric effect [7,8]. Motivated by their exotic electronic response, optical properties of TIs have also been investigated extensively [7–12]. In fact, a topological *magneto-optical* response has been identified: for thin-film TIs, Faraday and Kerr angles are predicted to be universal and quantized in units of the fine structure constant [7,13–18]. Recent experiments have directly measured these quantized values [19]. In general, electronic and optical response can be understood from the linear response theory appropriate to systems in or near equilibrium. However, the investigation of far-from-equilibrium physics in topological systems has remained elusive.

In this Letter, we consider a thin TI film at finite temperature, weakly coupled to ferromagnetic insulators on both top and bottom surfaces of the TI, immersed in an environment at zero temperature. Ferromagnetic insulators and the bulk of the TI are assumed to have a large intrinsic band gap and a negligible optical response. The TI radiates energy to the environment in a process that is similar to blackbody radiation; however, we demonstrate that the radiation of hot photons to the environment is strongly circularly polarized, and thus carries away angular momentum. As a result, the TI itself experiences a backaction torque that we show to be directly governed by the ac Hall conductivity. In particular, we investigate the universal nonequilibrium response of the TI to the temperature difference with the environment. Finally, we show that the observation of this effect should be comfortably within experimental reach.

*Model.*—The surface states of a TI are described by the Dirac-like Hamiltonian (with $\hbar = 1$) [20]

$$H = (-1)^L v(\sigma_x k_x + \sigma_y k_y) + \sigma_z \Delta, \qquad (1)$$

where $L = 0$, 1 denotes the TI's top or bottom surfaces parallel to the $x$-$y$ plane, $v$ is the Fermi velocity of the surface states, and $\sigma_i$ are the usual Pauli matrices. This minimal Hamiltonian should suffice at room temperature well below the bulk band gap. The first term in the Hamiltonian describes the gapless modes in the Dirac spectrum, while the last term ($\Delta > 0$) arises because the weak coupling to a ferromagnet breaks time-reversal symmetry [7,21]. Such proximity-induced ferromagnetism has been demonstrated experimentally [22–25]; see also Refs. [26,27]. We are ultimately interested in computing the heat radiation from the TI out of thermal equilibrium with the environment. To this end, we need to first characterize the electronic response of the TI which dictates its interaction with light. To determine the electronic response, we can use the Kubo formula at a finite temperature to find the conductivity tensor [28]

 

$$\sigma_{\alpha\beta}(\omega) = \sum_{\mathbf{k}} \sum_{nn'} \frac{f_{\mathbf{k}n} - f_{\mathbf{k}n'}}{\varepsilon_{\mathbf{k}n} - \varepsilon_{\mathbf{k}n'}} \frac{\langle \mathbf{k}n | j_\alpha | \mathbf{k}n' \rangle \langle \mathbf{k}n' | j_\beta | \mathbf{k}n \rangle}{\omega + \varepsilon_{\mathbf{k}n} - \varepsilon_{\mathbf{k}n'} + i\gamma},$$

where the current is $j_\alpha = \partial H / \partial k_\alpha = ev\sigma_\alpha$ with $\alpha = x, y$ as the spatial coordinates along the surface. The quantum numbers $\{\mathbf{k}, n = \mathrm{c/v}\}$ denote the momentum and conduction or valence bands, respectively. The energy spectrum is given by $\varepsilon_{\mathbf{k}\mathrm{c/v}} = \pm\sqrt{v^2\mathbf{k}^2 + \Delta^2}$ and $\gamma/2$ is the quasiparticle lifetime broadening. Also $f_{\mathbf{k}n} = [1 + \exp(\varepsilon_{\mathbf{k}n}/T)]^{-1}$ is the Fermi factor at a temperature $T$ for band $n$; the chemical potential is set to zero. In the limit of $T \to 0$ and $\omega \to 0$, only the Hall conductivity is nonvanishing, $\sigma_{xy} = e^2/(4\pi\hbar)$. At finite frequencies, $\sigma_{xy}(\omega)$ gives the ac Hall conductivity [13,18]. A first inspection of conductivity reveals that it is peaked at the interband absorption threshold, $\omega = 2\Delta$, which is the onset of the resonant coupling of the valence and conduction bands. These peaks are more pronounced at low temperatures, but survive even at higher temperatures comparable to or even larger that the gap size; see Fig. 1(a). For convenience, we shall choose units in which $\hbar = c = k_B = 1$ unless stated otherwise.

The TI is coupled to light in a peculiar fashion determined by its surface conductivity [13,18,19,29]. For a thin TI slab, we can ignore the bulk which has a much larger gap than the surface. We nevertheless consider the slab to be sufficiently thick to prevent bottom and top surface states from hybridizing; a thickness $\gtrsim 10$ nm typically suffices [22–25]. With these assumptions, an incident wave is reflected by a single effective surface whose conductivity is the sum of that from both surfaces. As a first step, consider a normally incident wave. Linearly polarized light is reflected off of the TI to a superposition of the two linear polarizations. However, right (+) or left (−) circular polarization is reflected as the same polarization with amplitude [13,18]

$$R_\pm(\omega) \approx -4\pi[\sigma_{xx}(\omega) \pm i\sigma_{xy}(\omega)]. \tag{2}$$

Here, $\sigma_{xx/xy}$ denote the conductivity of either the top or bottom surface, while an overall factor of 2 is due to the contribution from both surfaces [13,18]. The above reflection matrices are known to give rise to universal Kerr and Faraday effects that characterize the *phase* of the scattered wave [13–15,19]. To determine radiation, we should first characterize the absorptive properties of the TI which are determined by the *amplitude*, rather than the phase, of the scattering matrix. Indeed the scattering matrix shows an interesting feature: near $\omega = 2\Delta$, right-circularly polarized light (along the $z$ direction) exhibits resonant behavior, while left-circularly polarized light barely interacts with the TI. To illustrate this point, we have plotted the real part of $\sigma_\pm = \sigma_{xx} \pm i\sigma_{xy}$ as a function of $\omega$ and at several temperatures in Fig. 1. Note that $\mathrm{Re}\sigma_{xx}$ and $\mathrm{Im}\sigma_{xy}$ (the only ones entering $\mathrm{Re}\sigma_\pm$) give the corresponding dissipative components of the conductivity tensor. These will be particularly relevant as radiation, accompanied by an increase of entropy, is intimately tied to dissipation.

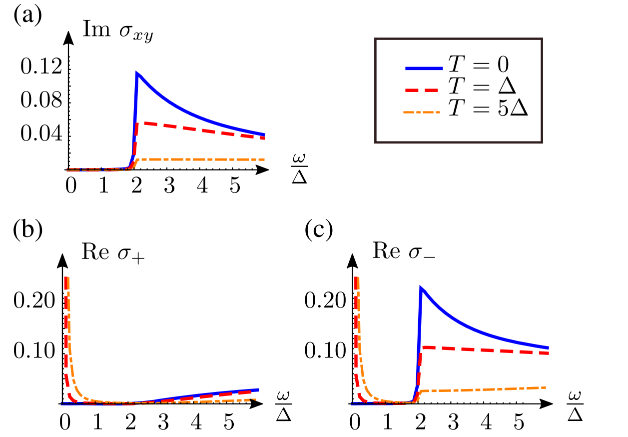


FIG. 1. Dissipative components of conductivity in units of $e^2/\hbar$ as a function of $\omega$ for several temperatures and $\gamma/\Delta = 0.01$. (a) The dissipative part of Hall conductivity $\mathrm{Im}\sigma_{xy}$ exhibits a resonant feature at the interband threshold $\omega = 2\Delta$. This quantity directly determines angular momentum radiation from the TI out of thermal equilibrium. (b), (c) The reflection matrices at normal incidence for the circular polarizations are proportional to $\sigma_\pm = \sigma_{xx} \pm i\sigma_{xy}$. The absorption of light by the TI is determined by the dissipative (real) parts of $\sigma_\pm$ as plotted in this figure. Only one polarization is resonant at the threshold resulting in a strongly polarized radiation; see text for the explanation.

The resonant feature of only one polarization follows from the strong spin-orbit coupling of the TI. In the region near $k_x = k_y = 0$, the Hamiltonian is simply $H \approx \sigma_z\Delta$, and thus the top of the valence band is occupied by spin-$|\downarrow\rangle$ electrons, while the bottom of the conduction band corresponds to unoccupied spin-$|\uparrow\rangle$ electrons. Thus, at zero temperature, the spin can only increase by one unit at the interband threshold. In other words, only a photon with a positive angular momentum along the $z$ direction can be absorbed, in which case a jump in the density of excited states at $\omega = 2\Delta$ gives rise to the resonant feature. At nonzero temperatures, the resonant feature smoothes out, but nevertheless persists.

*Radiation of angular momentum.*—Electromagnetic waves carry energy, but they can also carry angular momentum. The angular momentum distribution of electromagnetic fields follows the standard definition of angular momentum as $\mathbf{L} = \int_{\mathrm{vol}} \mathbf{x} \times \mathbf{S}$ with $\mathbf{x}$ the position vector and $\mathbf{S} = (1/4\pi)\mathbf{E} \times \mathbf{B}$ the Poynting vector defining the energy current ($c = 1$ and Gaussian units are chosen for convenience). Much like how the Poynting vector quantifies the flow of energy, change of angular momentum can be related to the *flux* of a certain tensor. In a compact four-vector notation, the conservation of energy can be deduced from $\partial_\nu T^{\mu\nu} = 0$ (summation over repeated indices is assumed). This equation implies that energy density $T^{00} = (1/8\pi)(\mathbf{E}^2 + \mathbf{B}^2)$ changes at a rate given by $T^{i0}$, which is simply the Poynting vector. Similarly, angular momentum conservation follows from $\partial_\lambda m^{\mu\nu\lambda} = 0$, where $m^{\mu\nu\lambda} = x^\mu T^{\nu\lambda} - x^\nu T^{\mu\lambda}$ is a rank-3 tensor [30]. The angular momentum due to rotation in the $i$-$j$ plane is given by $L^{ij} = \int_{\mathbf{x}} m^{ij0}$ with Roman indices denoting spatial coordinates. The rate of angular momentum (density) transfer along the $l$ direction is then given by the tensor $m^{ijl}$. Specifically, the quantity $N_z = \int dxdy m^{xyz} = \int dxdy[xT^{yz} - yT^{xz}]$ determines the rate at which the $z$ component of angular momentum is radiated along the $z$ direction. Identifying $T^{ij}$ as the Maxwell stress tensor, we find $N_z = (1/4\pi)\int dxdy[(\mathbf{x}\times\mathbf{E})_z E_z + (\mathbf{x}\times\mathbf{B})_z B_z]$; see the Supplemental Material [31].

To study the TI out of thermal equilibrium with its environment, we need a framework suited to far-from-equilibrium situations. A powerful framework is provided by the Keldysh formalism. Within this framework, the dynamics is expressed on a closed time contour with two branches along the forward and backward directions in time. It is often convenient to work in the Keldysh basis where each field finds two, *classical* and *quantum*, components. We express the dynamics in terms of the gauge field $\mathbf{A}$ in a gauge where the scalar potential is set to zero [28]; the electric and magnetic fields are then described as $\mathbf{E} = -\partial_t \mathbf{A}$ and $\mathbf{B} = \nabla \times \mathbf{A}$. The path integral is then a sum over both classical and quantum field configurations $Z = \int D\mathbf{A}^{cl} D\mathbf{A}^{q} \exp(iS_K[\mathbf{A}^{cl}, \mathbf{A}^{q}])$ with $S_K$ being the Keldysh action; $\mathbf{A}^{cl/q} \equiv (\mathbf{A}^f \pm \mathbf{A}^b)/\sqrt{2}$, where $f$, $b$ refer to the forward and backward branches of the closed contour, respectively. For a thin TI, we can write the action describing the interaction between the TI and the electromagnetic field vacuum in terms of circularly polarized components $A_\pm \equiv (A_x \pm iA_y)/\sqrt{2}$ as [32]

$$S_{\mathrm{TI}} = \sum_{s=\pm} \int \frac{d\omega}{2\pi} \int_{\mathrm{TI}} \begin{pmatrix} A_s^{cl*} & A_s^{q*} \end{pmatrix} \begin{pmatrix} 0 & \Pi_s^A \\ \Pi_s^R & \Pi_s^K \end{pmatrix} \begin{pmatrix} A_s^{cl} \\ A_s^{q} \end{pmatrix}. \tag{3}$$

Notice that $S_{\mathrm{TI}}$ is proportional to the fine structure constant, $\alpha = e^2/(\hbar c) \approx 1/137$; therefore the TI is weakly coupled to the environment. This equation describes the interaction of the gauge field with the TI surface: $\Pi_\pm^C$ indicate the current-current correlation tensors (cross-correlations between the two circularly polarized basis states vanish due to the underlying symmetry); $C = R, A, K$ correspond to the retarded, advanced, and Keldysh components, respectively. The components of the current-current correlation functions can be identified from the conductivity tensor. In general, we have $\sigma_{\alpha\beta}(\omega) = (i/\omega)\Pi_{\alpha\beta}^R(\omega)$. The indices $\alpha$, $\beta$ denote the spatial directions, which can be converted to the circular-polarization basis via $\Pi_\pm^R = \Pi_{xx}^R \mp i\Pi_{xy}^R$, where we have implicitly used the relations $\Pi_{xx}^R = \Pi_{yy}^R$ and $\Pi_{xy}^R = -\Pi_{yx}^R$ owing to the underlying symmetries of the TI. The advanced and retarded components are related to each other via time reversal operation as $\Pi_\pm^A = \Pi_\pm^{R*}$. To identify the Keldysh component of the current-current correlation $\Pi_\pm^K$, note that the currents on the surface are locally in equilibrium with a reservoir at temperature $T$; thus a local equilibrium condition is dictated by the fluctuation-dissipation theorem [32]: $\Pi_\pm^K = 4[n(\omega, T) + 1/2]\mathrm{Im}\Pi_\pm^R$; the function $n(\omega, T)$ denotes the Bose-Einstein distribution at temperature $T$. In particular, we note $\mathrm{Im}\Pi_+^R - \mathrm{Im}\Pi_-^R = 4\omega \mathrm{Im}\sigma_{xy}(\omega)$ with an additional factor of 2 included due to the contribution of both top and bottom surfaces (see the Supplemental Material [31]). This relation will appear shortly in deriving the angular momentum radiation from the TI.

To obtain the angular momentum radiation, we should compute the expectation value $\langle N_z \rangle$, which characterizes the total angular momentum flux along the $z$ direction; we consider the surface at a constant $z > 0$ but will multiply the final result by a factor of 2 to account for the radiation to both $z \to \pm\infty$. We also note that this radiation is absent in equilibrium and is directly a consequence of the TI being out of thermal equilibrium with the environment. Since the coupling of the TI to the electromagnetic field in the environment is proportional to $\alpha$, one should expect the radiation to be of the same order. To this order (i.e., within Born approximation), we compute $\langle N_z \rangle \approx i\langle N_z S_{\mathrm{TI}} \rangle_0$, where the subscript 0 indicates that the average is computed over fluctuations in free space in the absence of the TI. We obtain

$$\langle N_z \rangle = \frac{2A}{\pi} \sum_{\pm} \int_0^\infty d\omega n(\omega, T) \mathrm{Im}\Pi_\pm^R \langle\langle N_z \rangle\rangle_\pm, \tag{4}$$

where the double bracket $\langle\langle \cdot \rangle\rangle$ is defined as follows. Consider a bilinear operator $O = XY$ where $X$ and $Y$ are (different components of) the vector field or derivatives thereof; we then define $\langle\langle XY \rangle\rangle_\pm \equiv \mathrm{Re}[\langle X^{cl} A_\pm^{q*} \rangle_0 \langle Y^{cl*} A_\pm^{q} \rangle_0]$, where the frequency ($\omega$) dependence is implicit. Each two-point correlation function then represents the (retarded or advanced) electrodynamic Green's function in free space. A straightforward manipulation of Green's functions yields a simple expression $\langle\langle N_z \rangle\rangle_\pm = \pm\omega/3$. We note in passing that the above equation can be easily extended to a situation where the vacuum is at a nonzero temperature $T_{\mathrm{env}}$ by replacing $n(\omega, T)$ by the difference $n(\omega, T) - n(\omega, T_{\mathrm{env}})$; clearly, there is no net radiation in thermal equilibrium when $T = T_{\mathrm{env}}$. Putting these terms together and using the previously noted relation $\mathrm{Im}\Pi_+ - \mathrm{Im}\Pi_- = 4\omega \mathrm{Im}\sigma_{xy}$, we find the total angular momentum radiation as (restoring units of $\hbar$ and $c$)

$$\langle N_z^{\mathrm{tot}} \rangle = 2\langle N_z \rangle = -\frac{16\hbar A}{3\pi c^3} \int_0^\infty d\omega \frac{\omega^2}{e^{\hbar\omega/T} - 1} \mathrm{Im}\sigma_{xy}. \tag{5}$$

An overall factor of 2 accounts for the total radiation to both $z \to \pm\infty$ as promised. More details of this calculation are reported in the Supplemental Material [31]. With our conventions ($\Delta > 0$), we have $\mathrm{Im}\sigma_{xy} > 0$ and thus the total angular momentum carried away from the object is strictly negative. As a result, the TI itself absorbs an influx of positive angular momentum per unit time; in other words, it experiences a positive *torque* due to the emitted radiation. The torque can also be understood by adopting a different perspective where the object is heated up initially and is then isolated from the thermal bath. Thermally populated phonons will then exchange energy with electrons; however, they can only do so if they also exchange angular momentum since the excitation of an electron from the valence to the conduction band requires an increase of angular momentum. The excess of electronic angular momentum is eventually radiated away, while, in the process, phonons gain a net (negative) angular momentum. A (positive) external torque should be exerted to maintain the TI at rest. Remarkably, Eq. (5) directly links the radiation of angular momentum by the TI to its (ac) Hall conductivity; cf. Fig. 1(a). Hall conductivity has originally described the chiral *electronic* response to an applied electric field, a phenomenon which also finds an *optical* counterpart in the form of Kerr effect. However, Eq. (5) offers a new interpretation where Hall conductivity governs a chiral *mechanical* response as a toque that is exerted on the TI due to the back action of angular momentum radiation.

Next we compute the total torque on the TI assuming a relatively clean system when $\gamma$ is vanishingly small. In this limit, we find the dissipative part of Hall conductivity as $\mathrm{Im}\sigma_{xy} = (e^2/\hbar)\Theta(\omega - 2\Delta)[\Delta \tanh(\hbar\omega/4T)/4\omega]$. This quantity is zero for frequencies smaller than the band gap, as expected. The torque, i.e., the back action of angular momentum radiation, can be now evaluated as

$$\mathrm{Torque} = -\langle N_z^{\mathrm{tot}}\rangle = \frac{\hbar\alpha A\Delta^3}{c^2} g\left(\frac{T}{\hbar\Delta}\right), \qquad (6)$$

where $g$ is a scaling function of $T/(\hbar\Delta)$ defined by $g(x) = 4/(3\pi)\int_2^\infty dz z/[1+\exp(z/2x)]^2$. This function can be computed analytically in terms of polylogarithms (see the Supplemental Material [31]); however, we find it more illuminating to discuss its scaling properties. At high temperatures $T \gg \hbar\Delta$, we find $g(x) \sim ax^2$ with the coefficient $a = 4(\pi^2 - 12\log 2)/(9\pi) \approx 0.22$. Therefore, at high temperatures, the torque scales quadratically with temperature. At low temperatures, however, the radiation is exponentially suppressed in the gap size $\sim e^{-2\hbar\Delta/T}$ as the dissipative component of Hall conductivity is vanishing within the band gap; see Fig. 2. It is worth mentioning that fluctuation-induced effects in equilibrium have been studied extensively in the presence of topological materials [33–39]. In particular, it is found that the force between two TI slabs is proportional to $\alpha^2$. This scaling can be contrasted with our result for nonequilibrium torque $\sim\alpha$. In computing the torque, we have neglected the edges of the TI. Due to their gapless nature, they can give rise to a qualitatively different effect [40]. However, we can imagine a scenario where only the bulk of the material is heated, in which case our treatment remains valid.

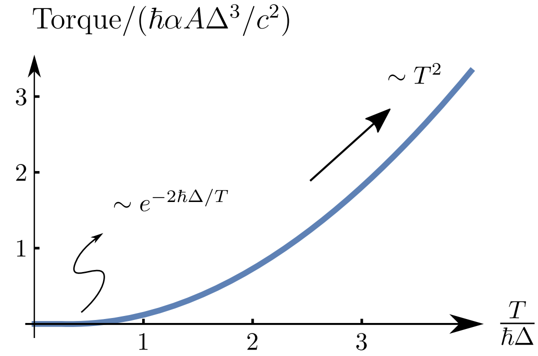


FIG. 2. The torque acting on the TI or the negative angular momentum radiated away as a function of temperature. At low temperatures, the torque is exponentially small in the gap size, while it rises sharply around $T \sim \Delta$ and increases quadratically with $T$ at high temperatures.

The effect reported in this work could also arise in gyrotropic materials in the presence of a static magnetic field which induces a nonzero $\sigma_{xy}$. However, a simple estimate shows that the resulting circular polarization is greatly suppressed at room temperature even for a large magnetic field ∼1 Tesla. On the other hand, strong spin-orbit coupling in the TI gives rise to a highly circularly polarized radiation even at temperatures larger than the surface gap; see the Supplemental Material [31]. We nevertheless remark that this effect is not unique to the TI, and can arise, for example, in materials involving Rashba surface states [41].

To estimate the strength of the torque, we take the surface gap $\Delta \sim 0.05$ eV [26,42,43] and the size of the TI slab in the mm range. To get a better sense of numbers, we compute the force that creates a given torque if applied at the boundary of the system. A simple estimate then shows that around $T \sim 2\Delta$, for example, this force is of the order of 1 pN, which is comfortably within the range of ultrasensitive force measurements [44]. Most radiation is emitted around the frequency set by temperature $\omega \sim T$ which, in our example, corresponds to the wavelength $\lambda \sim 1$ $\mu$m. This is large compared to the TI thickness ($d \sim 10$ nm), which justifies our assumption of a thin TI ($\lambda \gg d$). Another, perhaps more feasible, route to detecting this effect is to measure the polarization of emitted photons. For example, we can collect light emitted normal to the surface, convert circular into linear polarization with a quarter-wave plate, and guide it through a polarizing beam splitter to split horizontal and vertical polarizations. We can then measure the intensity at the two output ports of the polarizing beam splitter. This procedure can measure light emitted in a narrow frequency band at a specific angle; however, it provides a strong evidence for the polarization of the emitted radiation.

*Conclusion and outlook.*—We have studied a thin TI slab with the time reversal symmetry broken, and out of thermal equilibrium with its environment. The material is shown to emit thermal photons with a high degree of circular polarization, thus experiencing a fluctuation-driven torque. This Letter adds to the magnetoelectric and magneto-optic effects a magneto-mechanical component. This effect arises in the absence of incident light and is driven purely by fluctuations of the electromagnetic field inside and vacuum fluctuations outside the material. Extensions of this Letter to other materials such as Weyl semimetals [45,46] and Rashba surface states [41] are worthwhile. An interesting future direction is to fully investigate the gapless edge states out of thermal equilibrium with the environment.

We thank Mark Dykman, Peng Wei, and Liang Wu for comments on the manuscript. M. M. acknowledges support from NSF under Grant No. DMR-1912799 and start-up funding from Michigan State University. A. V. G. acknowledges support by AFOSR, ARO, the NSF PFCQC program, the DoE BES QIS program (Award No. DE-SC0019449), the DoE ASCR Quantum Testbed Pathfinder program (Award No. DE-SC0019040), ARL CDQI, NSF PFC at JQI, and ARO MURI. J. S. is supported by NSF-DMR-1555135 (CAREER), JQI-NSF-PFC (PHY1430094), and the Sloan research fellowship.

*Corresponding author.
maghrebi@pa.msu.edu

[1] C. L. Kane and E. J. Mele, Phys. Rev. Lett. **95**, 146802 (2005).
[2] L. Fu, C. L. Kane, and E. J. Mele, Phys. Rev. Lett. **98**, 106803 (2007).
[3] J. E. Moore and L. Balents, Phys. Rev. B **75**, 121306(R) (2007).
[4] M. Z. Hasan and C. L. Kane, Rev. Mod. Phys. **82**, 3045 (2010).
[5] M. Z. Hasan and J. E. Moore, Annu. Rev. Condens. Matter Phys. **2**, 55 (2011).
[6] X.-L. Qi and S.-C. Zhang, Rev. Mod. Phys. **83**, 1057 (2011).
[7] X.-L. Qi, T. L. Hughes, and S.-C. Zhang, Phys. Rev. B **78**, 195424 (2008).
[8] A. M. Essin, J. E. Moore, and D. Vanderbilt, Phys. Rev. Lett. **102**, 146805 (2009).
[9] A. B. Sushkov, G. S. Jenkins, D. C. Schmadel, N. P. Butch, J. Paglione, and H. D. Drew, Phys. Rev. B **82**, 125110 (2010).
[10] G. S. Jenkins, A. B. Sushkov, D. C. Schmadel, N. P. Butch, P. Syers, J. Paglione, and H. D. Drew, Phys. Rev. B **82**, 125120 (2010).
[11] J. N. Hancock, J. L. M. van Mechelen, A. B. Kuzmenko, D. van der Marel, C. Brüne, E. G. Novik, G. V. Astakhov, H. Buhmann, and L. W. Molenkamp, Phys. Rev. Lett. **107**, 136803 (2011).
[12] R. Valdés Aguilar, A. V. Stier, W. Liu, L. S. Bilbro, D. K. George, N. Bansal, L. Wu, J. Cerne, A. G. Markelz, S. Oh *et al.*, Phys. Rev. Lett. **108**, 087403 (2012).
[13] W.-K. Tse and A. H. MacDonald, Phys. Rev. Lett. **105**, 057401 (2010).
[14] W.-K. Tse and A. H. MacDonald, Phys. Rev. B **82**, 161104 (R) (2010).
[15] M. Z. Hasan, Physics **3**, 62 (2010).
[16] J. Maciejko, X.-L. Qi, H. D. Drew, and S.-C. Zhang, Phys. Rev. Lett. **105**, 166803 (2010).
[17] G. Tkachov and E. M. Hankiewicz, Phys. Rev. B **84**, 035405 (2011).
[18] W.-K. Tse and A. H. MacDonald, Phys. Rev. B **84**, 205327 (2011).
[19] L. Wu, M. Salehi, N. Koirala, J. Moon, S. Oh, and N. P. Armitage, Science **354**, 1124 (2016).
[20] H. Zhang, C.-X. Liu, X.-L. Qi, X. Dai, Z. Fang, and S.-C. Zhang, Nat. Phys. **5**, 438 (2009).
[21] D. Hsieh, Y. Xia, D. Qian, L. Wray, J. H. Dil, F. Meier, J. Osterwalder, L. Patthey, J. G. Checkelsky, N. P. Ong *et al.*, Nature (London) **460**, 1101 (2009).
[22] P. Wei, F. Katmis, B. A. Assaf, H. Steinberg, P. Jarillo-Herrero, D. Heiman, and J. S. Moodera, Phys. Rev. Lett. **110**, 186807 (2013).
[23] Q. I. Yang, M. Dolev, L. Zhang, J. Zhao, A. D. Fried, E. Schemm, M. Liu, A. Palevski, A. F. Marshall, S. H. Risbud *et al.*, Phys. Rev. B **88**, 081407(R) (2013).
[24] Y. Yu Wang and P. J. Burke, Appl. Phys. Lett. **103**, 052103 (2013).
[25] F. Katmis, V. Lauter, F. S. Nogueira, B. A. Assaf, M. E. Jamer, P. Wei, B. Satpati, J. W. Freeland, I. Eremin, D. Heiman *et al.*, Nature (London) **533**, 513 (2016).
[26] C.-Z. Chang, J. Zhang, X. Feng, J. Shen, Z. Zhang, M. Guo, K. Li, Y. Ou, P. Wei, L.-L. Wang *et al.*, Science **340**, 167 (2013).
[27] X.-L. Qi, Y.-S. Wu, and S.-C. Zhang, Phys. Rev. B **74**, 085308 (2006).
[28] G. D. Mahan, *Many-Particle Physics* (Springer Science & Business Media, New York, 2000).
[29] P. Di Pietro, F. M. Vitucci, D. Nicoletti, L. Baldassarre, P. Calvani, R. Cava, Y. S. Hor, U. Schade, and S. Lupi, Phys. Rev. B **86**, 045439 (2012).
[30] L. D. Landau and E. M. Lifshitz, *The Classical Theory of Fields* (Butterworth-Heinemann, Oxford, 1987), Vol. 2.
[31] See Supplemental Material at http://link.aps.org/supplemental/10.1103/PhysRevLett.123.055901 for details omitted from the main text.
[32] A. Kamenev, *Field Theory of Non-Equilibrium Systems* (Cambridge University Press, Cambridge, England, 2011).
[33] A. G. Grushin and A. Cortijo, Phys. Rev. Lett. **106**, 020403 (2011).
[34] A. G. Grushin, P. Rodriguez-Lopez, and A. Cortijo, Phys. Rev. B **84**, 045119 (2011).
[35] W.-K. Tse and A. H. MacDonald, Phys. Rev. Lett. **109**, 236806 (2012).
[36] W. Nie, R. Zeng, Y. Lan, and S. Zhu, Phys. Rev. B **88**, 085421 (2013).
[37] P. Rodriguez-Lopez and A. G. Grushin, Phys. Rev. Lett. **112**, 056804 (2014).
[38] A. A. Allocca, J. H. Wilson, and V. Galitski, Phys. Rev. B **90**, 075420 (2014).
[39] J. H. Wilson, A. A. Allocca, and V. M. Galitski, Phys. Rev. B **91**, 235115 (2015).

[40] S. Ryu, J. E. Moore, and A. W. W. Ludwig, Phys. Rev. B **85**, 045104 (2012).

[41] N. Nagaosa, J. Sinova, S. Onoda, A. H. MacDonald, and N. P. Ong, Rev. Mod. Phys. **82**, 1539 (2010).

[42] L. A. Wray, S.-Y. Xu, Y. Xia, D. Hsieh, A. V. Fedorov, Y. S. Hor, R. J. Cava, A. Bansil, H. Lin, and M. Z. Hasan, Nat. Phys. **7**, 32 (2011).

[43] S.-Y. Xu, M. Neupane, C. Liu, D. Zhang, A. Richardella, L. Andrew Wray, N. Alidoust, M. Leandersson, T. Balasubramanian, J. Sánchez-Barriga *et al.*, Nat. Phys. **8**, 616 (2012).

[44] M. Li, H. X. Tang, and M. L. Roukes, Nat. Nanotechnol. **2**, 114 (2007).

[45] B. Q. Lv, H. M. Weng, B. B. Fu, X. P. Wang, H. Miao, J. Ma, P. Richard, X. C. Huang, L. X. Zhao, G. F. Chen *et al.*, Phys. Rev. X **5**, 031013 (2015).

[46] S.-Y. Xu, I. Belopolski, N. Alidoust, M. Neupane, G. Bian, C. Zhang, R. Sankar, G. Chang, Z. Yuan, C.-C. Lee *et al.*, Science **349**, 613 (2015).